HHS Public Access

Author manuscript

*Biol Psychiatry Cogn Neurosci Neuroimaging*. Author manuscript; available in PMC 2024 March 14.

Published in final edited form as:

*Biol Psychiatry Cogn Neurosci Neuroimaging*. 2024 February ; 9(2): 207–216. doi:10.1016/j.bpsc.2023.08.002.

# Prenatal Exposure to Maternal Mood Entropy Is Associated With a Weakened and Inflexible Salience Network in Adolescence

**Robert J. Jirsaraie**,
Center for the Neurobiology of Learning and Memory, University of California, Irvine, Irvine, California

Department of Neurobiology and Behavior, University of California, Irvine, Irvine, California

**Anton M. Palma**,
Department of Statistics, University of California, Irvine, Irvine, California

**Steven L. Small**,
School of Behavioral and Brain Sciences, University of Texas at Dallas, Dallas, Texas

**Curt A. Sandman**,
Department of Psychiatry and Human Behavior, University of California, Irvine, Irvine, California

**Elysia Poggi Davis**,
Department of Psychology, University of Denver, Denver, Colorado

Department of Pediatrics, University of California, Irvine, Irvine, California

**Tallie Z. Baram**,
Center for the Neurobiology of Learning and Memory, University of California, Irvine, Irvine, California

Department of Pediatrics, University of California, Irvine, Irvine, California

Department of Anatomy and Neurobiology, University of California, Irvine, Irvine, California

**Hal Stern**,
Department of Statistics, University of California, Irvine, Irvine, California

**Laura M. Glynn**,
Department of Psychology, Chapman University, Orange, California

**Michael A. Yassa**
Center for the Neurobiology of Learning and Memory, University of California, Irvine, Irvine, California

Department of Neurobiology and Behavior, University of California, Irvine, Irvine, California

Department of Psychiatry and Human Behavior, University of California, Irvine, Irvine, California

Address correspondence to Laura M. Glynn, Ph.D., at lglynn@chapman.edu, or Michael A. Yassa, Ph.D., at myassa@uci.edu.

DISCLOSURES

The authors report no biomedical financial interests or potential conflicts of interest.

Supplementary material cited in this article is available online at https://doi.org/10.1016/j.bpsc.2023.08.002.

Department of Anatomy and Neurobiology, University of California, Irvine, Irvine, California

## Abstract

**BACKGROUND:** Fetal exposure to maternal mood dysregulation influences child cognitive and emotional development, which may have long-lasting implications for mental health. However, the neurobiological alterations associated with this dimension of adversity have yet to be explored. Here, we tested the hypothesis that fetal exposure to entropy, a novel index of dysregulated maternal mood, would predict the integrity of the salience network, which is involved in emotional processing.

**METHODS:** A sample of 138 child-mother pairs (70 females) participated in this prospective longitudinal study. Maternal negative mood level and entropy (an index of variable and unpredictable mood) were assessed 5 times during pregnancy. Adolescents engaged in a functional magnetic resonance imaging task that was acquired between 2 resting-state scans. Changes in network integrity were analyzed using mixed-effect and latent growth curve models. The amplitude of low frequency fluctuations was analyzed to corroborate findings.

**RESULTS:** Prenatal maternal mood entropy, but not mood level, was associated with salience network integrity. Both prenatal negative mood level and entropy were associated with the amplitude of low frequency fluctuations of the salience network. Latent class analysis yielded 2 profiles based on changes in network integrity across all functional magnetic resonance imaging sequences. The profile that exhibited little variation in network connectivity (i.e., inflexibility) consisted of adolescents who were exposed to higher negative maternal mood levels and more entropy.

**CONCLUSIONS:** These findings suggest that fetal exposure to maternal mood dysregulation is associated with a weakened and inflexible salience network. More broadly, they identify maternal mood entropy as a novel marker of early adversity that exhibits long-lasting associations with offspring brain development.

Exposure to adversity in early life exerts profound impacts on the developing brain, with lifelong consequences for mental health. In particular, the prenatal period is a sensitive window in time during which in utero signals shape neurodevelopmental trajectories (1,2). Among those signals, maternal mood states are well-established determinants of child cognitive and emotional development (3). Numerous studies have demonstrated that prenatal maternal depression, anxiety, and stress are each uniquely associated with alterations in offspring brain structure and connectivity, conferring risk across many forms of child psychopathology (4–6). More specifically, these studies indicated that the neural circuitry that links the amygdala and prefrontal cortex can be disrupted by negative maternal mood states during fetal life. Diffusion imaging studies have revealed microstructural differences in the white matter tracts that connect the amygdala and prefrontal cortex among children with higher exposures to prenatal maternal depression (7), anxiety (6,8), and stress (9). These findings are consistent with structural imaging studies that have reported alterations in subcortical limbic structures (10) and executive prefrontal regions (2,7,11,12).

In contrast to brain structure, little is known about how brain function is impacted by prenatal exposures. To date, we are aware of only 2 functional neuroimaging studies that

have been conducted with children exposed to prenatal maternal depression, and they yielded mixed results (13,14). One study found that in 6-month-old infants of mothers with depression, the amygdala had stronger connectivity with the whole brain (13). By contrast, the other study found that in 8-month-old infants of mothers with depression, the amygdala was less functionally integrated with executive and affective regions (14). Although functional imaging investigations of prenatal adversity exposures are scarce, more literature has examined the associations between postnatal adversity and child brain development (5,15), yielding 2 recurring findings. First, studies using resting-state magnetic resonance imaging (MRI) have documented relationships between early-life adversity and salience network connectivity (16–18). Second, studies using task-based MRI demonstrated that adolescents who have been exposed to adversity in early life tend to exhibit greater brain activation when viewing fearful faces, specifically in regions comprising the salience network. This is in agreement with evidence that the salience network facilitates socioemotional regulation (19) and switching between attention states (20).

In addition to the extensively documented forms of early-life adversity that shape developmental trajectories of mental health (e.g., poverty, abuse, parental psychopathology), accumulating evidence indicates that unpredictability in the parental and home environment shapes the developing brain beginning during the fetal period (21–27). With direct relevance to maternal mood and mental health, 2 recent studies found that in addition to mood level (e.g., extremity of symptoms) or valence (e.g., positive or negative), a new indicator of maternal mood dysregulation, mood entropy (an index of unpredictable mood), was associated with multiple developmental outcomes, including infant negative affectivity, child cognitive development, and adolescent anxiety and depressive symptoms (28,29). The current study extends previous research by evaluating the association between both prenatal maternal negative mood level and mood entropy and functional brain networks.

Leveraging data from a prospective longitudinal cohort of children and adolescents (ages 10.8–16.8 years) who were followed from the prenatal period, the current study aimed at understanding the functional neural markers that are uniquely associated with fetal exposures to maternal mood dysregulation (i.e., level and entropy). Participants in this study completed an emotional processing MRI scan that was acquired in between 2 resting-state MRI scans, enabling us to evaluate brain function across 3 conditions. Given the established literature linking postnatal adversity to the salience network, we hypothesized that children with prenatal exposure to higher levels of dysregulated maternal mood (level and entropy) would also exhibit individual differences in the salience network. To test this hypothesis, we analyzed multiple functional MRI (fMRI) properties of the salience network, including task-evoked activation when passively viewing fearful faces in contrast to neutral ones (30), how uniquely interconnected the salience network was throughout the brain (31), and its degree of spontaneous activation within each fMRI sequence (32). Lastly, we analyzed changes between resting-state and task-evoked processing or how brain networks dynamically reconfigured in response to task demands, which we operalizationaled herein as the flexiability of a given network (33). Past research has suggested that the flexibility of networks can be measured via moment-to-moment fluctuations in connectivity across rest and task conditions and that this within-subject variability is associated with cognitive processing (34) and socioemotional outcomes (35).

# METHODS AND MATERIALS

## Study Overview

Pregnant women were recruited during the first trimester of pregnancy, and maternal mood was assessed 5 times during gestation (at 15, 19, 25, 31, and 36 weeks). Children (70 females; mean age: 13.5 years, age range: 10.8–16.8 years) completed structural and fMRI scanning during adolescence. Additionally, maternal mood was assessed concurrently with the MRI scanning session. The recruitment criteria and data collection process for this cohort of 138 mother-child pairs are summarized in the Supplement and have been extensively documented in previous reports (28,29). Demographic information about these mother-child pairs was collected using self-report assessments (Table 1).

## Assessment of Dysregulated Maternal Mood

**Negative Mood Level.—**At each prenatal assessment, mothers completed widely used and validated measures to assess depressive symptoms (Center for Epidemiological Studies Depression Scale - Short Form) (36), state anxiety (State-Trait Personality Inventory) (37), pregnancy-specific anxiety (38), and perceived stress (Perceived Stress Scale) (39). Each questionnaire was scored conventionally as an index of maternal negative mood level during pregnancy. To create a single composite index of maternal prenatal mood level, scores on the 4 scales were standardized and averaged within each time point, and those means were subsequently averaged across all 5 time points, which we refer to herein as mood level.

**Mood Entropy.—**As has been described in detail elsewhere (28,29), an index of maternal mood entropy was computed by applying Shannon's entropy to the distribution of responses on each of the mood questionnaires (e.g., mood entropy; the open-source R function is available at https://contecenter.uci.edu/measuring-maternal-mood/). This approach involves a quantification of the unpredictability of the item-by-item responses to assessments of mood. The responses within a single assessment are tabulated over the items within each scale into probability distributions based on the relative frequency of each response choice, and these distributions represent empirical estimates of the propensity of a participant to respond across items in a consistent way. Therefore, mood entropy represents the degree of predictability of the item-specific response. For example, a participant who generally reports never feeling sad or always enjoying life on the Center for Epidemiological Studies Depression Scale would be considered very predictable and thus have a very low entropy score, whereas a participant who completes the Center for Epidemiological Studies Depression Scale items entirely at random would be assigned a very high entropy score. As with prenatal maternal mood level, mood entropy scores were averaged across scales within each time point, and those means were averaged across time. Previous research has shown that this index of unpredictable mood is positively associated with daily ecological, momentary assessments of maternal mood variability and also predicts infant, child, and adolescent neurodevelopmental outcomes (28,29). Importantly, computed entropy scores from assessments unrelated to mood (e.g., physical activity) are not predictive of offspring developmental outcomes (6,7). Mood entropy scores were similarly computed and averaged across depression, perceived stress, and state anxiety scores from the maternal assessments at the adolescent MRI.

### Image Acquisition and fMRI Tasks

All brain scans were acquired using a Philips 3T MRI scanner equipped with a 32-channel head coil at the University of California, Irvine. Blood oxygen level–dependent (BOLD) fMRI acquisition used whole-brain, single-band, echo-planar images with the following parameters: 3-$mm^3$ isotropic resolution, repetition time = 2000 ms, echo time = 20 ms, 51 interleaved slice acquisition, field of view = 192 × 192 × 153 $mm^3$, flip angle = 71°, matrix = 62 × 64, SENSE parallel reduction factor of 2. Data collection began after the fourth image to allow for stabilization of the MR signal. Prior to collecting fMRI data, structural brain imaging was completed using a T1-weighted sequence with the following parameters: 1-$mm^3$ isotropic resolution, repetition time = 8 ms, echo time = 3.7 ms, 208 slices, field of view = 256 × 256 × 208 $mm^3$, flip angle = 8, matrix = 256 × 210.

As part of this scanning session, participants completed 3 consecutive fMRI scans. The first scan accessed participants' baseline BOLD activity while at rest (REST-1), during which they were instructed to keep their eyes fixated on a crosshair that was displayed in the center of a screen. Next, participants engaged in an emotional processing task (TASK) that elicits activation within the amygdala (40–42). This task consists of passively viewing faces that have either neutral or fearful expressions and are randomly presented for 350 ms in an event-related design (Figure S1). Lastly, participants completed a second resting-state task (REST-2) that was identical to the first resting sequence. Each resting-state sequence consisted of 150 volumes, whereas the task-based sequence contained 130 volumes, resulting in a total of 430 images across the entire fMRI scanning session, which lasted for 14 minutes and 20 seconds.

### Image Processing and Quality Assurance

FMRIPrep (version 20.1.1) (43) was used to preprocess all 3 fMRI sequences. Each subject's T1-weighted image was used as a reference throughout the workflow after images were corrected for intensity inhomogeneities (N4Bias-FieldCorrection) (44), skull-stripped (antsBrainExtraction) (45), and segmented based on tissue type (FSL-FAST) (46). Spatial normalization was completed by nonlinearly registering and resampling scans to the International Consortium for Brain Mapping 152 nonlinear asymmetrical template (antsRegistration) (47). Because field maps were not collected, distortion correction was estimated using Advanced Normalization Tool's symmetrical normalization (48). Head-motion parameters were estimated before any spatiotemporal filtering (FSL-MCFLIRT) (49). Automatic removal of motion artifacts using independent component analysis (ICA) (ICA-based automatic removal of motion artifacts) (50) was performed on the normalized BOLD time series, which were spatially smoothed by a 6-mm Gaussian kernel.

The XCP imaging pipeline (version 1.2.1) (51) was used to apply additional denoising methods and evaluate image quality. Every preprocessed fMRI sequence underwent Butterworth filtering to demean and detrend each time series; therefore, only signals in the 0.01 to 0.08 Hz range were retained. Nuisance regression analysis was applied to remove the mean time series of the white matter and cerebrospinal fluid. The ICA-based automatic removal of motion artifacts pipeline was most effective at attenuating motion-related artifacts while preserving temporal degrees of freedom (Figure S2). This assessment

was based on its ability to attenuate distance-dependent artifacts as quantified by the correlation between functional connectivity and Euclidean distances in a 264 node-network (52). Despite the presence of head motion in our sample (Figure S3), our denoising strategy yielded data that had few artifacts compared with previously reported benchmarks (53).

### Parcellating Brain Networks Using ICA

The FSL-MELODIC (version 3.15) (54) software package was used to perform spatial group ICA. Multisession temporal concatenation was applied only to the REST-1 time series so that components would be derived from resting baseline activity and not a mixture of task-evoked signals. Multiple ICA resolutions (8–24 networks) were examined based on 2 criteria: 1) keeping well-known intrinsic connectivity networks intact (55) and 2) reducing dimensionality to limit the number of comparisons. Based on these criteria, the 12-component solution was selected, with all networks confirmed by visual inspection. The resulting images were 3-dimensional, but each component was mapped onto a surface using BrainNet Viewer (56) for visualization purposes (Figure S4). Only the 10 nonartifact components were included in the whole-brain analyses to assess whether effects were specific to the salience network.

### Task-Related Activation During Passive Viewing of Fearful Faces

FSL-FEAT (version 6.0) (30) was used to model task-evoked brain activity while viewing neutral and fearful faces. These 2 types of events and their temporal derivatives were included as regressors in the time series model where gamma convolution was applied. A single contrast was derived to measure the amount of activation while viewing fearful faces compared with neutral ones. This contrast was used to determine which clusters had more activation when viewing fearful faces as opposed to neutral ones for all subjects. The resulting group-level activation map was created using FLAME stage 1 (57), which only retained clusters of voxels that had $z$ values larger than 3.1 and survived a cluster-corrected significance threshold of .05.

### Integrity of Intrinsic Connectivity Networks

Dual regression analysis (version 0.5) (31) was used to generate subject-specific spatial maps that were derived from the group-level ICA templates that were derived across all participants in this sample. This multivariate method takes a participant’s fully processed 4-dimensional fMRI sequence and extracts the average signal for all 12 ICA templates. The resulting time series captures the unique signal associated with each ICA template, which is subsequently regressed onto every voxel in the participant’s preprocessed sequences (58). The final output from this workflow is a set of beta-weight maps that capture individual differences in the magnitude and shape of each ICA template. Rapid changes in the topography of functional networks occur during childhood and adolescence (59), making it important to account for individual variation in the shape of functional networks. Following previous studies (15,60), the average beta weight from each subject-specific map was used to represent the integrity of a given ICA component. This procedure was repeated independently for all 3 fMRI sequences.

### Amplitude of Low-Frequency Fluctuations

Amplitude of low-frequency fluctuations (ALFF) is defined as the total power within the low frequency range, and thus it indexes the strength or intensity of low-frequency oscillations. This measure may be a proxy for spontaneous brain activation because it is susceptible to changes in environmental stimuli (61) and cognitive demands (62). Rhythmic activity of low-frequency fluctuations is the basis for determining the functional connectivity between nodes. Here, it was utilized as a proxy to estimate variability in activation of the salience network. Accordingly, we computed the ALFF for each network by taking the sum of amplitudes from frequencies ranging from 0.01 to 0.08 Hz. As was true for network integrity, we computed the ALFF for each of the 3 fMRI sequences that were acquired.

### Rationale for Statistical Analyses

Previous functional brain studies have only investigated whether individuals who were exposed to prenatal adversity exhibited differences in brain function while at rest. In contrast, individual differences in task-based processing is one of the most commonly reported neural abnormalities associated with various forms of postnatal adversity. Therefore, it is not clear from previous literature whether prenatal negative maternal mood level would also be associated with task-based processing or whether significant differences would only be apparent during resting state. Furthermore, the functional brain signatures of prenatal maternal mood entropy have yet to be examined altogether. Here, we had the unique opportunity to evaluate the network dynamics both while at rest and during a task. More specifically, we took 2 data-driven approaches to understand brain-behavior relations: 1) we conducted moderation analyses to understand whether the relationship between salience network integrity and maternal mood differed between task conditions, and 2) we performed latent growth curve modeling to identify groups of participants whose changes in network integrity were similar throughout the entire fMRI scanning session and subsequently evaluated whether exposure to prenatal adversity predicted membership in these groups. These approaches yielded complementary information because moderation analysis informs us about individual differences between task conditions, and latent growth curve modeling reflects within-subject changes in network dynamics across all fMRI sequences. Lastly, we attempted to extend our findings by analyzing individual differences in the ALFF because this metric represents changes in brain activation within a given fMRI sequence. We believe that this comprehensive approach was essential to narrowing down which biomarkers were uniquely associated with prenatal exposure to maternal mood level and entropy. Furthermore, such analyses were useful for identifying which experimental condition (resting-state vs. task-based) was most likely to elicit the largest differences.

### Statistical Analyses

Statistical analyses were completed using R (version 3.6), and the code is publicly available: https://github.com/yassalab/ConteCenterScripts/tree/master/Conte-One/scripts/analyses/IntraFlux. The following 6 analytical approaches were used to understand the neural mechanisms underlying exposure to prenatal maternal negative mood level and entropy. Unless otherwise specified, all the analyses that follow were conducted with separate models to evaluate mood level and entropy independently (see equations in

the Supplement). First, linear regression analyses were used to assess whether prenatal mood level and entropy were associated with brain activation in response to fearful faces during the task-based MRI. Second, mixed-effect models with random intercepts for each participant (package lme4, version 1.1) (63) were used to determine whether individual differences in network integrity varied as a function of prenatal maternal mood level and entropy. Interaction analyses were conducted to evaluate whether relationships between prenatal mood (level and entropy) and salience integrity were dependent on fMRI task conditions (prenatal mood × fMRI time point). Third, latent class mixture modeling (R package lcmm, version 1.9.2) (64) was used to identify common patterns of within-subject changes in network integrity across all 3 fMRI sequences. Post hoc tests were performed to determine whether the resulting latent profiles differed by exposure to prenatal maternal mood level and entropy. Fourth, mixed-effect models were also used to analyze the ALFF and corroborate findings observed with network integrity. Fifth, given that there is a well-established literature documenting sex-specific influences of early-life experience on neurodevelopment (65), sex was examined as a possible moderator of the relationships between prenatal maternal mood (level and entropy) and potential neural correlates (prenatal mood × sex). Sixth, sensitivity analyses were performed to understand the unique contributions of exposure to prenatal maternal mood level versus entropy and prenatal versus postnatal mood entropy and to account for potential confounding influences related to image quality or socioeconomic status. To assess whether the observed relationships were specific to the salience network, brainwide analyses were conducted on the 9 remaining intrinsic connectivity networks (Figure S4). For these analyses, Benjamini-Hochberg false discovery rate correction (66) was applied to account for multiple comparisons.

## RESULTS

### The Emotional Processing Task Increased Activation of Regions Within the Salience Network

Cluster-based fMRI analyses across all participants showed that fearful faces elicited activation in regions that comprise the salience network, consistent with results of previous studies (40). More specifically, clusters of activation were localized within the left amygdala, occipital pole, lingual gyrus cingulate, left inferior frontal gyrus, right middle frontal gyrus, and right orbitofrontal cortex (Figure 1).

Salience network activation in response to fearful faces did not vary as a function of prenatal maternal mood level ($\beta = 0.07$, $t_{133} = 0.76$, $p = .45$) or entropy ($\beta = 0.08$, $t_{133} = 0.88$, $p = .38$). This also was true for other intrinsic connectivity networks ($q > 0.34$).

### Prenatal Maternal Mood Entropy Predicted Integration of the Salience Network

Dual regression analysis was used to derive subject-specific spatial maps for each ICA network, thereby quantifying how uniquely interconnected a given network was throughout the brain (e.g., integrity). Across the 3 sequences, integrity of the salience network was negatively associated with mood entropy ($\beta = -0.11$, $t_{407} = -22.09$, $p = .04$) (Figure 2) but not mood level ($\beta = -0.05$, $t_{407} = -1.02$, $p = .31$). Moderation analyses indicated that the relationship between salience integrity and mood entropy did not differ among each of

the fMRI sequences (β = 0.08, $t_{403}$ = 1.22, $p$ = .23), suggesting that this association was independent of task-related processing. Analysis of all intrinsic connectivity networks did not uncover any additional relationships that survived multiple comparison correction for either mood level ($q$ > 0.19) or mood entropy ($q$ < 0.20).

### Prenatal Maternal Mood Entropy Predicted Inflexibility of the Salience Network

Our 3-scan design allowed the assessment of changes between resting-state and task-evoked processing. Such changes between fMRI sequences can represent the flexibility of functional networks or the ability to dynamically reconfigure networks to address task demands. Latent class mixture modeling was used to analyze within-subject changes in network integrity across all fMRI sequences, which revealed that a 2-class solution fit the data best (Table S1). This 2-class solution yielded a group of participants whose salience networks were relatively invariable (i.e., inflexible) across all 3 fMRI sequences compared with a second group whose networks demonstrated greater flexibility (Figure 3). As shown in Table 2, participants in the inflexible group had greater exposure to negative mood (d = 0.53, $t_{407}$ = 5.31, $p$ < .001) and higher maternal mood entropy during gestation (d = −20.58, $t_{407}$ = 5.39, $p$ < .001).

### Prenatal Maternal Mood Entropy Predicted Decreased ALFF of the Salience Network

While the measure of network flexibility above assesses changes across sequences, it does not capture spontaneous fluctuations in the BOLD fMRI signal within a given scan. Thus, we conducted a set of analyses to determine whether the invariability of the salience network would also be reflected uniformly through reductions in its ALFF. Accordingly, we found that adolescents who were in the inflexible latent profile also displayed substantial reductions in the ALFF both while at rest and during a task (Figure 4). In addition to these group differences between latent profiles, mixed-effect models indicated that the ALFF of the salience network was inversely associated with prenatal maternal mood level (β = −0.15, $t_{407}$ = −1.96, $p$ = .05) and entropy (β = −0.19, $t_{407}$ = −2.43, $p$ = .01).

### No Evidence of Sex Differences

Inclusion of a sex × maternal mood interaction term in the models did not uncover any systematic differences between boys and girls for the effect of either prenatal maternal mood level or entropy (Table S2).

### Examining the Unique Contributions of Prenatal Maternal Mood Entropy

Despite the strong correlation between prenatal maternal mood level and entropy ($r$ = 0.75) (Figure S5), only entropy was reliably associated with both salience network integrity and the ALFF. To test the specificity of these associations, additional analyses were conducted that included both assessments of maternal mood as predictors concurrently. Prenatal maternal mood entropy remained a statistically significant predictor of salience network integrity (β = −0.16, $t_{406}$ = −2.0, $p$ = .04), but its relationship with the ALFF did not remain statistically significant (β = −0.17, $t_{406}$ = −1.43, $p$ = .15). Mood level was not associated with salience network integrity (β = −0.07, $t_{406}$ = 0.85, $p$ = .41) or ALFF (β = −0.03, $t_{406}$ = −0.21, $p$ = .83) in these analyses (Table S3). To determine whether the relationship

between the salience network and maternal mood entropy was specific to the prenatal period, we conducted an additional set of analyses with prenatal and postnatal mood entropy as predictors. We replicated the association between prenatal mood entropy and the ALFF of the salience network ($\beta = -0.20$, $t_{406} = -2.37$, $p = .02$), but the association with salience integrity did not remain statistically significant ($\beta = -0.10$, $t_{406} = -1.77$, $p = .08$). Despite a moderate correlation between prenatal and postnatal maternal mood unpredictability ($r = 0.39$), postnatal maternal mood entropy did not exhibit any relationships with any proprieties of the salience network (Table S4). Lastly, sensitivity analyses indicated that the relationship between mood entropy and the salience network did not change significantly when accounting for potential confounding influences of head motion or income-to-needs ratio (see the Supplement).

## DISCUSSION

These results provide evidence that fetal exposure to dysregulated maternal mood may alter the development of the salience network through a reduction in its integration and flexibility, with stronger associations observed for prenatal exposures to unpredictable maternal mood (entropy) than for negative mood level. These relations were specific to the salience network and did not manifest in other intrinsic connectivity networks. Results were reproduced using 2 distinct functional measures, which characterize different aspects of network dynamics while at rest and during tasks. Importantly, these findings were specific to prenatal exposures, as maternal mood entropy measured during adolescence did not predict salience network features, and the addition of postnatal mood entropy did not substantively alter the association between prenatal mood entropy and functional measures of the salience network. Overall, these findings suggest that reduced integration and flexibility of the salience network may be markers of fetal exposure to maternal mood entropy. It is possible that the reduction in flexibility is an indication that the network's ability to dynamically change and reconfigure its activity in response to external or internal stimuli is compromised. Indeed, the salience network plays a critical role in switching between mental states and exerting cognitive control (67). Disruptions to these brain-behavior relationships have been shown to be involved in several mental illnesses (68). Furthermore, such findings are consistent with work from our group showing that higher levels of prenatal maternal mood entropy were associated with poorer cognitive and emotional outcomes in the same prospective longitudinal sample of children (28,29). Altogether, these findings support the notion that intrauterine experience may shape the flexibility of the salience network and possibly confer risk for compromised mental health.

Contrary to expectations, prenatal exposure to maternal mood entropy was not associated with a heightened response toward fearful faces. Because past work using similar task-evoked activation detected associations with postnatal adversity exposures (40), it is possible that our findings may reflect a key difference in the functional correlates underlying prenatal adversity. Because this is the first neuroimaging study in which prenatal exposure to maternal mood entropy was investigated, it is important for subsequent research to investigate how its neural correlates may differ from other dimensions of adversity.

A primary objective of this study was to determine whether salience integrity was uniquely associated with fetal exposure to 2 related components of maternal mood dysregulation. Both maternal negative mood level and entropy, although related, were independently associated with properties of the salience network. However, entropy was the only predictor that persisted in regression models that included both variables. Thus, after accounting for other aspects of maternal mood severity (level and valence of symptoms), exposure to unpredictable mood during the gestational period appears to have unique contributions to offspring salience network integrity. This is consistent with the increasing recognition that unpredictability represents a distinct dimension of early-life experience that can alter neurodevelopmental trajectories (25,27,69) and builds on our group's previous work demonstrating that fetal exposure to unpredictable maternal mood is associated with child cognitive and emotional outcomes (28,29).

There are several strengths of this work. First, our longitudinal cohort with data collection beginning in the fetal period and continuing through adolescence allowed prospective examination of prenatal influences on neurodevelopment. Second, our assessments of maternal mood dysregulation were based on item-level responses across 4 distinct scales, which is a critical advantage for deriving more reliable metrics across time (70,71). For example, recent evidence suggests that concurrent examination of multiple indicators of maternal mood leads to improved prediction of internalizing and externalizing symptoms in early adolescence as compared to using a single scale (72). Additionally, using an ICA approach to deriving intrinsic connectivity networks provided parsimonious summaries of the high-dimensional imaging data, thereby limiting multiple comparisons and denoising motion-related components at the group level (73). Finally, we analyzed 3 fMRI sequences for each participant, which allowed us to assess multiple facets of brain function (74).

We also acknowledge a potential limitation of the current study. As with most studies conducted with children and adolescents, there is a higher level of within-scanner head movement than is typically found in adults. We used several correction techniques to mitigate the contamination caused by movement and compared the top-ranked denoising methods and settled on ICA-based automatic removal of motion artifacts as the technique that most effectively reduced distant-dependent artifacts (53). Additionally, we excluded approximately 20% of scans that exhibited the most movement and still replicated our key findings (see the Supplement). Thus, we are reasonably confident that the findings presented herein are not the result of motion-related confounds.

## Conclusions

Our results provide evidence that prenatal exposure to a novel index of maternal mood dysregulation, unpredictable maternal mood, is associated with a weakened and inflexible salience network during adolescence. More broadly, our findings underscore the need to consider mood entropy in addition to mood severity when examining influences of maternal mental health on child neurodevelopment and also further highlights the central role of maternal mental health in shaping the developing brain.

## Supplementary Material

Refer to Web version on PubMed Central for supplementary material.

## ACKNOWLEDGMENTS

This research was supported by the National Institutes of Health (Grant Nos. NS-41298, R01HD28413, R01HD51852, R01NS41298, and P50MH96889) and by National Science Foundation Graduate Research Fellowship Program (Grant Nos. DGE-2139839 and DGE-1745038), which provided additional funding support for RJJ.

We thank the families who participated in these projects. We also thank the dedicated staff at the Early Human and Lifespan Development Program and the Women and Children's Health and Well-Being Project.

## REFERENCES

1. Glynn LM, Baram TZ (2019): The influence of unpredictable, fragmented parental signals on the developing brain. Front Neuroendocrinol 53:100736. [PubMed: 30711600]
2. Demers CH, Bagonis MM, Al-Ali K, Garcia SE, Styner MA, Gilmore JH, et al. (2021): Exposure to prenatal maternal distress and infant white matter neurodevelopment. Dev Psychopathol 33:1526–1538. [PubMed: 35586027]
3. Sandman CA, Class QA, Glynn LM, Davis EP (2016): Chapter 13-Neurobehavioral disorders and developmental origins of health and disease. In: Rosenfeld CS, editor. The Epigenome and Developmental Origins of Health and Disease. Boston: Academic Press, 235–266.
4. Marečková K, Klasnja A, Bencurova P, Andrýsková L, Brázdil M, Paus T (2019): Prenatal stress, mood, and gray matter volume in young adulthood. Cereb Cortex 29:1244–1250. [PubMed: 29425268]
5. Jenness JL, Peverill M, Miller AB, Heleniak C, Robertson MM, Sambrook KA, et al. (2021): Alterations in neural circuits underlying emotion regulation following child maltreatment: a mechanism underlying trauma-related psychopathology. Psychol med 51:1880–1889. [PubMed: 32252835]
6. Demers CH, Aran Ö., Glynn LM, Davis EP (2021): Prenatal Programming of Neurodevelopment: Structural and Functional Changes. In: Wazana A, Székely E, Oberlander TF, editors. Prenatal Programming of Neurodevelopment: Structural and Functional Changes BT – Prenatal Stress and Child Development. Cham: Springer International Publishing, 193–242.
7. El Marroun H, Zou R, Muetzel RL, Jaddoe VW, Verhulst FC, White T, Tiemeier H (2018): Prenatal exposure to maternal and paternal depressive symptoms and white matter microstructure in children. Depress Anxiety 35:321–329. [PubMed: 29394520]
8. Dean DC 3rd, Planalp EM, Wooten W, Kecskemeti SR, Adluru N, Schmidt CK, et al. (2018): Association of prenatal maternal depression and anxiety symptoms with infant white matter microstructure. JAMA Pediatr 172:973–981. [PubMed: 30177999]
9. Sarkar S, Craig MC, Dell'Acqua F, O'Connor TG, Catani M, Deeley Q, et al. (2014): Prenatal stress and limbic-prefrontal white matter microstructure in children aged 6–9 years: A preliminary diffusion tensor imaging study. World J Biol Psychiatry 15:346–352. [PubMed: 24815522]
10. Wen DJ, Poh JS, Ni SN, Chong YS, Chen H, Kwek K, et al. (2017): Influences of prenatal and postnatal maternal depression on amygdala volume and microstructure in young children. Transl Psychiatry 7: e1103. [PubMed: 28440816]
11. Davis EP, Hankin BL, Glynn LM, Head K, Kim DJ, Sandman CA (2020): Prenatal maternal stress, child cortical thickness, and adolescent depressive symptoms. Child Dev 91:e432–e450. [PubMed: 31073997]
12. Sandman CA, Buss C, Head K, Davis EP (2015): Fetal exposure to maternal depressive symptoms is associated with cortical thickness in late childhood. Biol Psychiatry 77:324–334. [PubMed: 25129235]

13. Qiu A, Anh TT, Li Y, Chen H, Rifkin-Graboi A, Broekman BFP, et al. (2015): Prenatal maternal depression alters amygdala functional connectivity in 6-month-old infants. Transl Psychiatry 5:e508. [PubMed: 25689569]
14. Posner J, Cha J, Roy AK, Peterson BS, Bansal R, Gustafsson HC, et al. (2016): Alterations in amygdala–prefrontal circuits in infants exposed to prenatal maternal depression. Transl Psychiatry 6:e935. [PubMed: 27801896]
15. Ordaz SJ, LeMoult J, Colich NL, Prasad G, Pollak M, Popolizio M, et al. (2017): Ruminative brooding is associated with salience network coherence in early pubertal youth. Soc Cogn Affect Neurosci 12:298–310. [PubMed: 27633394]
16. Herzberg MP, Gunnar MR (2020): Early life stress and brain function: Activity and connectivity associated with processing emotion and reward. Neuroimage 209:116493. [PubMed: 31884055]
17. Thomason ME, Hamilton JP, Gotlib IH (2011): Stress-induced activation of the HPA axis predicts connectivity between subgenual cingulate and salience network during rest in adolescents. J Child Psychol Psychiatry 52:1026–1034. [PubMed: 21644985]
18. Marusak HA, Etkin A, Thomason ME (2015): Disrupted insula-based neural circuit organization and conflict interference in traumaexposed youth. Neuroimage Clin 8:516–525. [PubMed: 26199869]
19. Toller G, Brown J, Sollberger M, Shdo SM, Bouvet L, Sukhanov P, et al. (2018): Individual differences in socioemotional sensitivity are an index of salience network function. Cortex 103:211–223. [PubMed: 29656245]
20. Goulden N, Khusnulina A, Davis NJ, Bracewell RM, Bokde AL, McNulty JP, Mullins PG (2014): The salience network is responsible for switching between the default mode network and the central executive network: Replication from DCM. Neuroimage 99:180–190. [PubMed: 24862074]
21. Davis EP, Stout SA, Molet J, Vegetabile B, Glynn LM, Sandman CA, et al. (2017): Exposure to unpredictable maternal sensory signals influences cognitive development across species. Proc Natl Acad Sci USA 114:10390–10395. [PubMed: 28893979]
22. Birnie MT, Baram TZ (2022): Principles of emotional brain circuit maturation. Science 376:1055–1056. [PubMed: 35653483]
23. Davis EP, Korja R, Karlsson L, Glynn LM, Sandman CA, Vegetabile B, et al. (2019): Across continents and demographics, unpredictable maternal signals are associated with children's cognitive function. EBiomedicine 46:256–263. [PubMed: 31362905]
24. Glynn LM, Davis EP, Luby JL, Baram TZ, Sandman CA (2021): A predictable home environment may protect child mental health during the COVID-19 pandemic. Neurobiol Stress 14:100291. [PubMed: 33532520]
25. Glynn LM, Stern HS, Howland MA, Risbrough VB, Baker DG, Nievergelt CM, et al. (2019): Measuring novel antecedents of mental illness: The Questionnaire of Unpredictability in Childhood. Neuropsychopharmacology 44:876–882. [PubMed: 30470840]
26. Spadoni AD, Vinograd M, Cuccurazzu B, Torres K, Glynn LM, Davis EP, et al. (2022): Contribution of early-life unpredictability to neuropsychiatric symptom patterns in adulthood. Depress Anxiety 39:706–717. [PubMed: 35833573]
27. Granger SJ, Glynn LM, Sandman CA, Small SL, Obenaus A, Keator DB, et al. (2021): Aberrant maturation of the uncinate fasciculus follows exposure to unpredictable patterns of maternal signals. J Neurosci 41:1242–1250. [PubMed: 33328295]
28. Glynn LM, Howland MA, Sandman CA, Davis EP, Phelan M, Baram TZ, Stern HS (2018): Prenatal maternal mood patterns predict child temperament and adolescent mental health. J Affect Disord 228:83–90. [PubMed: 29241049]
29. Howland MA, Sandman CA, Davis EP, Stern HS, Phelan M, Baram TZ, Glynn LM (2021): Prenatal maternal mood entropy is associated with child neurodevelopment. Emotion 21:489–498. [PubMed: 32202848]
30. Woolrich MW, Ripley BD, Brady M, Smith SM (2001): Temporal autocorrelation in univariate linear modeling of FMRI data. Neuroimage 14:1370–1386. [PubMed: 11707093]
31. Nickerson LD, Smith SM, Öngür D, Beckmann CF (2017): Using dual regression to investigate network shape and amplitude in functional connectivity analyses. Front Neurosci 11:115–115. [PubMed: 28348512]

32. Zhang J, Liu DQ, Qian S, Qu X, Zhang P, Ding N, Zang YF (2023): The neural correlates of amplitude of low-frequency fluctuation: A multimodal resting-state MEG and fMRI–EEG study. Cereb Cortex 33:1119–1129. [PubMed: 35332917]
33. Ebisch SJH, Gallese V, Salone A, Martinotti G, di Iorio G, Mantini D, et al. (2018): Disrupted relationship between "resting state" connectivity and task-evoked activity during social perception in schizophrenia. Schizophr Res 193:370–376. [PubMed: 28735643]
34. Gonzalez-Castillo J, Bandettini PA (2018): Task-based dynamic functional connectivity: Recent findings and open questions. Neuroimage 180:526–533. [PubMed: 28780401]
35. Siffredi V, Liverani MC, Freitas LGA, Tadros D, Farouj Y, Borradori Tolsa C, et al. (2023): Large-scale brain network dynamics in very preterm children and relationship with socio-emotional outcomes: An exploratory study. Pediatr Res 93:2072–2080. [PubMed: 36329223]
36. Santor DA, Coyne JC (1997): Shortening the CES–D to improve its ability to detect cases of depression. Psychol Assess 9:233–243.
37. Spielberger CD, Gonzalez-Reigosa F, Martinez-Urrutia A, Natalicio LF, Natalicio DS (1971): The state-trait anxiety inventory. Revista Interamericana de Psicologia/Interamerican journal of psychology 5.
38. Rini CK, Dunkel-Schetter C, Wadhwa PD, Sandman CA (1999): Psychological adaptation and birth outcomes: The role of personal resources, stress, and sociocultural context in pregnancy. Health Psychol 18:333–345. [PubMed: 10431934]
39. Cohen S, Kamarck T, Mermelstein R (1983): A global measure of perceived stress. J Health Soc Behav 24:385–396. [PubMed: 6668417]
40. Fusar-Poli P, Placentino A, Carletti F, Landi P, Allen P, Surguladze S, et al. (2009): Functional atlas of emotional faces processing: A voxelbased meta-analysis of 105 functional magnetic resonance imaging studies. J Psychiatry Neurosci 34:418–432. [PubMed: 19949718]
41. Baird AA, Gruber SA, Fein DA, Maas LC, Steingard RJ, Renshaw PF, et al. (1999): Functional magnetic resonance imaging of facial affect recognition in children and adolescents. J Am Acad Child Adolesc Psychiatry 38:195–199. [PubMed: 9951219]
42. Thomas KM, Drevets WC, Dahl RE, Ryan ND, Birmaher B, Eccard CH, et al. (2001): Amygdala response to fearful faces in anxious and depressed children. Arch Gen Psychiatry 58:1057–1063. [PubMed: 11695953]
43. Esteban O, Markiewicz CJ, Blair RW, Moodie CA, Isik AI, Erramuzpe A, et al. (2019): fMRIPrep: A robust preprocessing pipeline for functional MRI. Nat Methods 16:111–116. [PubMed: 30532080]
44. Tustison NJ, Avants BB, Cook PA, Zheng Y, Egan A, Yushkevich PA, Gee JC (2010): N4ITK: Improved N3 bias correction. IEEE Trans Med Imaging 29:1310–1320. [PubMed: 20378467]
45. Tustison NJ, Cook PA, Holbrook AJ, Johnson HJ, Muschelli J, Devenyi GA, et al. (2021): The ANTsX ecosystem for quantitative biological and medical imaging. Sci Rep 11:9068. [PubMed: 33907199]
46. Jenkinson M (2003): Fast, automated, N-dimensional phase-unwrapping algorithm. Magn Reson Med 49:193–197. [PubMed: 12509838]
47. Fonov VS, Evans AC, McKinstry RC, Almli CR, Collins DL (2009): Unbiased nonlinear average age-appropriate brain templates from birth to adulthood. Neuroimage 47:S102.
48. Wang S, Peterson DJ, Gatenby JC, Li W, Grabowski TJ, Madhyastha TM (2017): Evaluation of field map and nonlinear registration methods for correction of susceptibility artifacts in diffusion MRI. Front Neuroinform 11:17. [PubMed: 28270762]
49. Jenkinson M, Bannister P, Brady M, Smith S (2002): Improved optimization for the robust and accurate linear registration and motion correction of brain images. NeuroImage 17:825–841. [PubMed: 12377157]
50. Pruim RHR, Mennes M, van Rooij D, Llera A, Buitelaar JK, Beckmann CF (2015): ICA-AROMA: A robust ICA-based strategy for removing motion artifacts from fMRI data. Neuroimage 112:267–277. [PubMed: 25770991]
51. Ciric R, Rosen AFG, Erus G, Cieslak M, Adebimpe A, Cook PA, et al. (2018): Mitigating head motion artifact in functional connectivity MRI. Nat Protoc 13:2801–2826. [PubMed: 30446748]

52. Power JD, Cohen AL, Nelson SM, Wig GS, Barnes KA, Church JA, et al. (2011): Functional network organization of the human brain. Neuron 72:665–678. [PubMed: 22099467]
53. Ciric R, Wolf DH, Power JD, Roalf DR, Baum GL, Ruparel K, et al. (2017): Benchmarking of participant-level confound regression strategies for the control of motion artifact in studies of functional connectivity. Neuroimage 154:174–187. [PubMed: 28302591]
54. Beckmann CF, Smith SM (2004): Probabilistic independent component analysis for functional magnetic resonance imaging. IEEE Trans Med Imaging 23:137–152. [PubMed: 14964560]
55. Garrett AS, Pliszka SR (2020): Neuroimaging of intrinsic connectivity networks: A robust method for assessing functional brain organization in psychiatric disorders. Braz J Psychiatry 42:1–2. [PubMed: 32022161]
56. Xia M, Wang J, He Y (2013): BrainNet Viewer: A network visualization Tool for human brain connectomics. PLoS One 8:e68910. [PubMed: 23861951]
57. Woolrich MW, Behrens TEJ, Beckmann CF, Jenkinson M, Smith SM (2004): Multilevel linear modelling for FMRI group analysis using Bayesian inference. Neuroimage 21:1732–1747. [PubMed: 15050594]
58. Zuo XN, Kelly C, Adelstein JS, Klein DF, Castellanos FX, Milham MP (2010): Reliable intrinsic connectivity networks: Test–retest evaluation using ICA and dual regression approach. NeuroImage 49:2163–2177. [PubMed: 19896537]
59. Cui Z, Li H, Xia CH, Larsen B, Adebimpe A, Baum GL, et al. (2020): Individual variation in functional topography of association networks in youth. Neuron 106:340–353.e8. [PubMed: 32078800]
60. Rohr CS, Arora A, Cho IYK, Katlariwala P, Dimond D, Dewey D, Bray S (2018): Functional network integration and attention skills in young children. Dev Cogn Neurosci 30:200–211. [PubMed: 29587178]
61. Yang Y, Zhong N, Imamura K, Lu S, Li M, Zhou H, et al. (2016): Task and resting-state fMRI reveal altered salience responses to positive stimuli in patients with major depressive disorder. PLoS One 11:e0155092. [PubMed: 27192082]
62. Gur RC, Butler ER, Moore TM, Rosen AFG, Ruparel K, Satterthwaite TD, et al. (2021): Structural and functional brain parameters related to cognitive performance across development: Replication and extension of the parieto-frontal integration theory in a single sample. Cereb Cortex 31:1444–1463. [PubMed: 33119049]
63. Bates D, Mächler M, Bolker B, Walker S (2015): Fitting linear mixed-effects models using lme4. J Stat Softw 67:1–48.
64. Proust-Lima C, Philipps V, Liquet B (2017): Estimation of Extended Mixed Models Using Latent Classes and Latent Processes: The R package lcmm. J Stat Soft 78:1–56.
65. De Bellis MD, Keshavan MS, Beers SR, Hall J, Frustaci K, Masalehdan A, et al. (2001): Sex differences in brain maturation during childhood and adolescence. Cereb Cortex 11:552–557. [PubMed: 11375916]
66. Thissen D, Steinberg L, Kuang D (2002): Quick and easy implementation of the Benjamini–Hochberg procedure for controlling the false positive rate in multiple comparisons. J Educ Behav Stat 27:77–83.
67. Snyder W, Uddin LQ, Nomi JS (2021): Dynamic functional connectivity profile of the salience network across the life span. Hum Brain Mapp 42:4740–4749. [PubMed: 34312945]
68. Wei M, Qin J, Yan R, Bi K, Liu C, Yao Z, Lu Q (2017): Abnormal dynamic community structure of the salience network in depression. J Magn Reson Imaging 45:1135–1143. [PubMed: 27533068]
69. Baram TZ, Davis EP, Obenaus A, Sandman CA, Small SL, Solodkin A, Stern H (2012): Fragmentation and unpredictability of early-life experience in mental disorders. Am J Psychiatry 169:907–915. [PubMed: 22885631]
70. Kessler RC, Chiu WT, Demler O, Merikangas KR, Walters EE (2005): Prevalence, severity, and comorbidity of 12-month DSM-IV disorders in the National comorbidity Survey Replication. Arch Gen Psychiatry 62:617–627. [PubMed: 15939839]

71. Snyder HR, Young JF, Hankin BL (2019): Chronic stress exposure and generation are related to the P-factor and externalizing specific psychopathology in youth. J Clin Child Adolesc Psychol 48:306–315. [PubMed: 28541762]

72. Bailey NA, Irwin JL, Davis EP, Sandman CA, Glynn LM (2023): Patterns of maternal distress from pregnancy through childhood predict psychopathology during early adolescence. Child Psychiatry Hum Dev 54:470–480. [PubMed: 34626290]

73. Eklund A, Nichols TE, Knutsson H (2016): Cluster failure: Why fMRI inferences for spatial extent have inflated false-positive rates. Proc Natl Acad Sci USA 113:7900–7905. [PubMed: 27357684]

74. Hasson U, Nusbaum HC, Small SL (2009): Task-dependent organization of brain regions active during rest. Proc Natl Acad Sci USA 106:10841–10846. [PubMed: 19541656]

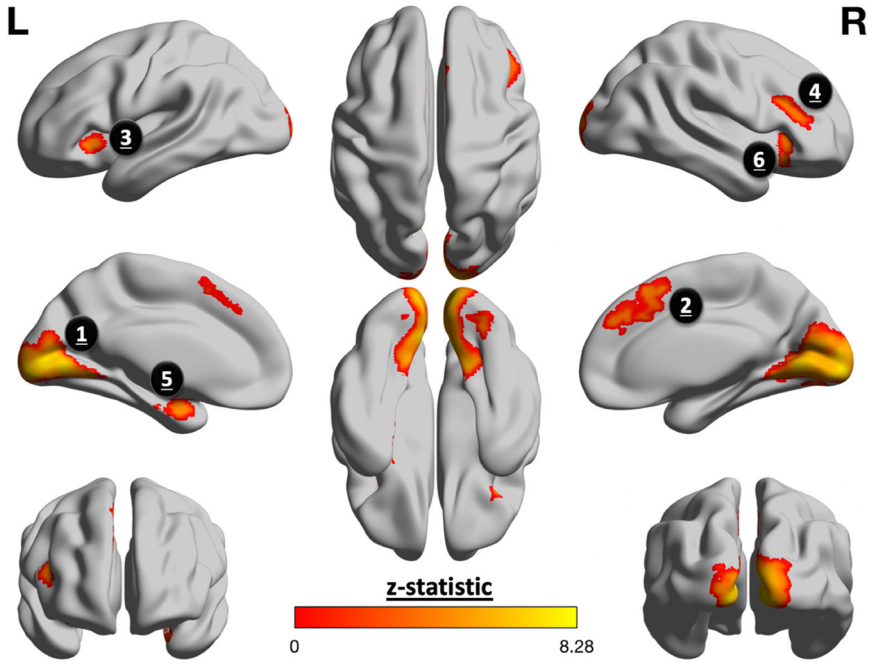


**Figure 1.**

Fearful faces elicited greater activation in salience processing regions. Group-level analyses of task-evoked activation yielded 6 clusters that were significantly more active for fearful faces than neutral ones. The following is a list of each cluster ordered from biggest to smallest, with parentheses to denote its corresponding number of voxels and *z* score, respectively: 1) lingual gyrus and occipital pole ($n = 9427$, $z = 8.29$); 2) cingulate gyrus ($n = 637$, $z = 5.65$); 3) left (L) inferior frontal gyrus ($n = 465$, $z = 5.34$); 4) right (R) middle frontal gyrus ($n = 250$, $z = 4.65$); 5) left amygdala ($n = 215$, $z = 5.84$); 6) left inferior frontal gyrus ($n = 164$, $z = 4.68$).

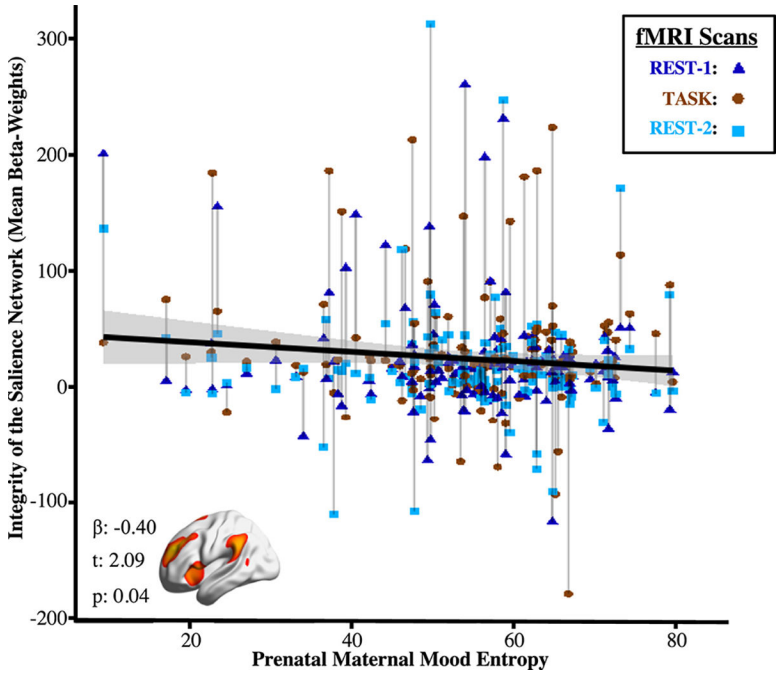


**Figure 2.**

Prenatal maternal mood entropy was negatively associated with integrity of the salience network across functional magnetic resonance imaging (fMRI) sequences. Integrity was derived from person-specific spatial maps for each intrinsic connectivity network. Brainwide analyses suggested that significant relationships were only detected with integrity of the salience network; relationships with all other intrinsic connectivity networks were nonsignificant.

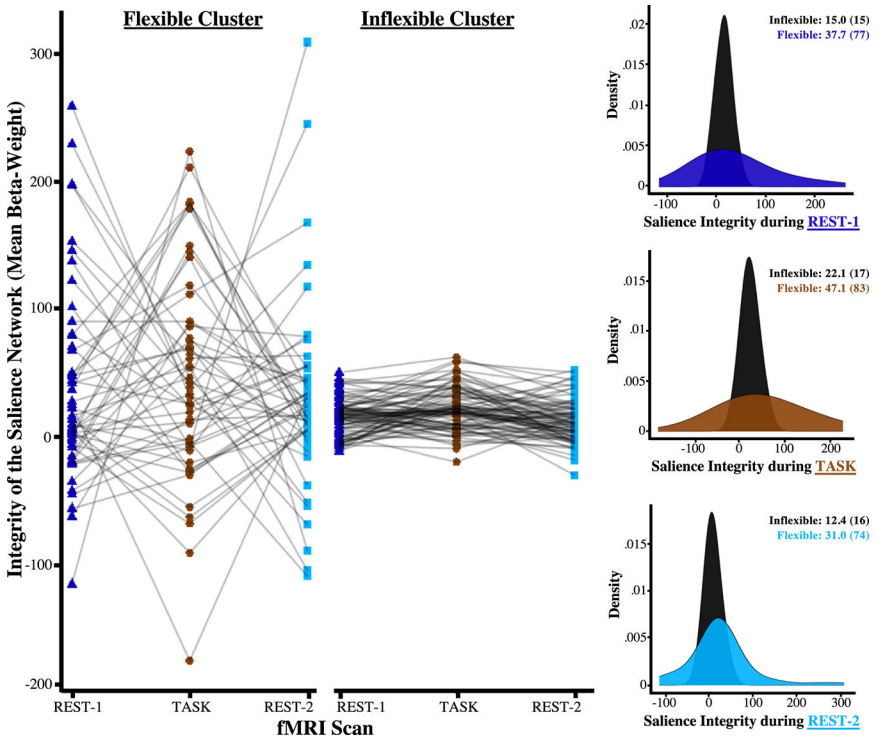


**Figure 3.**

Data-driven clustering of network integrity derived 2 latent profiles that were differentiated by their degree of change between functional magnetic resonance imaging (fMRI) sequences. Participants engaged in a task-based scan that was acquired in between 2 resting-state scans. This experimental design enabled us to cluster participants based on changes in brain connectivity across the entire fMRI scanning session. A 2-class solution fit the data best, yielding 2 clusters that were best distinguished by the degree of fluctuations in brain integrity. Specifically, the histograms demonstrate that the integrity of the salience network differed significantly with these 2 clusters because the cluster displayed in black exhibited relatively few changes to the MRI task conditions. Adolescents in the inflexible cluster were exposed to significantly higher negative maternal mood level and more mood entropy during gestation.

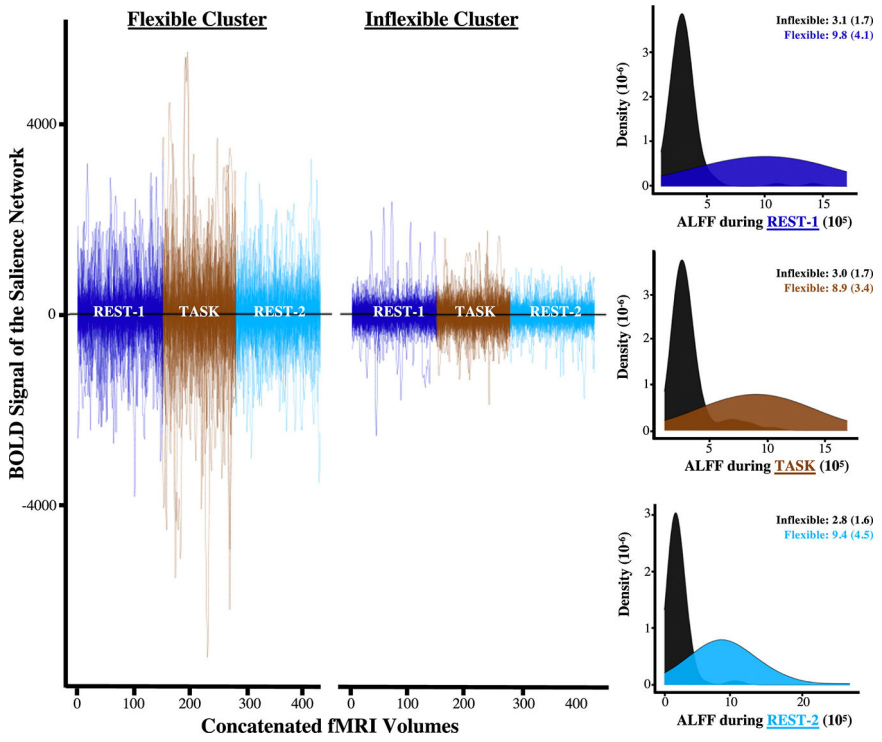


**Figure 4.**

Amplitudes of low-frequency fluctuations (ALFFs) mapped onto patterns of change that were derived from fluctuations in network integrity. Each line in the scatterplot above represents the fully processed blood oxygen level–dependent (BOLD) signal for a given participant, which is concatenated and color coded by the order in which functional magnetic resonance imaging (fMRI) sequences were collected. The scatterplot illustrates converging evidence that the BOLD fluctuations of the salience network were smaller for the inflexible latent profile. The histograms also highlight the fact that such differences between latent profiles were apparent within each sequence and across the entire fMRI scanning session.

**Table 1.**

Demographic and Other Characteristics of Study Participants

| Variable of Interest | Entire Sample, *N* = 138 |
|---|---|
| Age at Scan, Years, Mean | 13.5 |
| Sex, Female, % | 50.70% |
| Maternal Race/Ethnicity, % | |
| Asian | 14.50% |
| Black | 8.00% |
| Latina | 30.40% |
| Non-Hispanic White | 38.40% |
| Other | 8.70% |
| Education, % | |
| High school or less | 15.90% |
| Some college, associate or vocational degree | 37.70% |
| 4-year college degree | 31.20% |
| Graduate degree | 14.50% |
| Maternal Characteristics | |
| Maternal age, years, mean | 30 |
| Annual household income, USD, mean | $62,190 |
| Cohabitation with child’s father, yes, % | 85.50% |
| Birth order, first-born, % | 47.80% |
| Length of gestation, weeks, mean | 39.28 |

**Table 2.**

Intraindividual Changes in Network Integrity Across fMRI Sequences Yielded Two Latent Profiles That Differed by Prenatal Maternal Mood Level and Entropy

| Variable of Interest | Entire Sample, *N* = 138 | Flexible Cluster, *n* = 51 | Inflexible Cluster, *n* = 87 | Statistic | *p* Value |
|---|---|---|---|---|---|
| Age at Scan, Years | 13.5 (1.7) | 12.9 (1.5) | 13.9 (1.7) | 6.03 | <.001 |
| Sex, Female, % | 50.70% | 55% | 48% | 1.43 | 0.231 |
| Head Motion, mm | 0.36 (0.4) | 0.41 (0.6) | 0.32 (0.4) | 1.54 | 0.199 |
| Prenatal Mood Level | −0.1 (0.8) | −0.4 (0.8) | 0.02 (0.8) | 5.31 | <.001 |
| Prenatal Mood Entropy | 55.2 (13.1) | 50.6 (14.4) | 57.9 (11.5) | 5.39 | <.001 |
| Salience Integrity Beta Weight | 24.7 (50.1) | 38.6 (77.8) | 16.5 (16.4) | 3.46 | <.001 |
| Salience ALFF in Units of 1 Million | 5.36 (4.1) | 9.38 (4.0) | 3.01 (1.7) | 18.7 | <.001 |